TABLE 3. Univariate and Multivariate Analysis in the Resection Group

	Univariate Analysis		Multivariate Analysis	
Independent Factor	HR (95% CI)	*P*	HR (95% CI)	*P*
Depth of tumor invasion	2.33 (1.56-3.69)	< .0001	1.45 (0.82-2.69)	.204
Lymph node metastasis	2.60 (1.80-4.04)	< .0001	1.53 (0.91-2.69)	.114
Distant metastasis	3.85 (1.11-10.28)	.035	0.87 (0.23-2.59)	.807
Lymphatic invasion	10.41 (3.05-65.08)	< .0001	1.73 (0.33-13.90)	.541
Vessel invasion	7.53 (2.58-31.99)	< .0001	1.62 (0.39-9.07)	.526
CTCs	2.77 (1.81-4.18)	< .0001	1.73 (1.08-2.77)	.024

Abbreviations: CI, confidence interval; CTCs, circulating tumor cells; HR, hazard ratio.

TABLE 4. Nonresectable Factors in the Nonresectable Group

	No. With CTCs		
Nonresectable Factor	Positive	Negative	Incidence of CTCs, %
Liver metastasis	9	7	56.3
Lung metastasis	0	2	0
Bone metastasis	4	1	80
Brain metastasis	2	0	100
Peritoneal dissemination	40	23	63.5
Lymph node metastasis	12	12	50
Direct invasion to peripheral organs	2	3	40

Abbreviations: CTCs, circulating tumor cells.

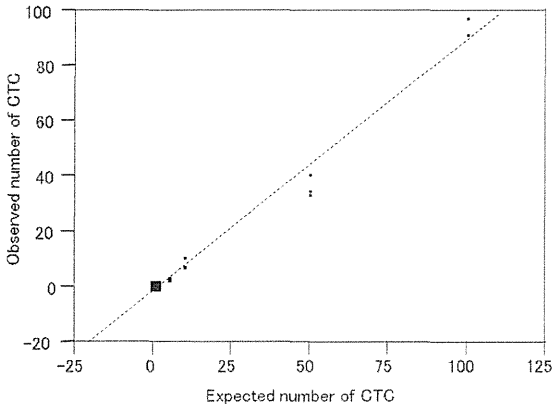

Figure 5. Regression analysis of the number of observed tumor cells versus the number of expected tumor cells produced a correlation coefficient (R^2) of 0.985. Even a single cell spiked into the samples was detected using this system.

number of observed tumor cells versus the number of expected tumor cells produced a correlation coefficient (R^2) of 0.985. Even a single cell spiked into the samples was detected using this system.

DISCUSSION

CTCs measured with the CellSearch system and clinical correlation of the results were analyzed in 251 patients with gastric adenocarcinoma. The system was sensitive, and the results were correlated with relapse-free survival, the 5-year survival rate, and the overall survival rate in all patients, including the resection group and the nonresectable group. Although previous studies have reported the presence of CTCs determined by RT-PCR, reports of the morphologic detection of CTCs are few.[15-19] Furthermore, ours was a large-scale, prospective study that enrolled 265 patients with gastric cancer. To our knowledge, this is the first longitudinal analysis evaluating CTCs using the CellSearch system in such patients.

In Japan, almost all patients who have stage II or III tumors after undergoing gastrectomy receive adjuvant chemotherapy in the form of oral S-1 according to data from the Adjuvant Chemotherapy Trial of TS-1 for Gastric Cancer (ACTS-GC).[20] However, ≥60% of patients at this stage do not have a recurrence without adjuvant chemotherapy. If recurrence after surgery can be predicted, then information regarding CTCs could help patients avoid unnecessary adjuvant chemotherapy. This distinction is necessary to determine whether or not patients are eligible for curative resection. The measurement of CTCs in gastric cancer will be useful for determining treatment strategies if more accurate staging of the patient can be performed. Moreover, patients with gastric cancer who have CTCs should receive neoadjuvant chemotherapy before they undergo surgery.

Patients who had breast cancer, prostate cancer, or colorectal cancer with hematogenous metastasis had a high incidence of CTCs according to several reports.[12,13,21] However, no significant correlation between positive CTCs and hematogenous distant metastasis in gastric cancer has been demonstrated. In the current study, peritoneal dissemination was the most frequently observed pattern of recurrence. The detection of CTCs may be a useful diagnostic tool for predicting

peritoneal dissemination, which is difficult to detect on imaging studies, such as computed tomography, ultrasonography, and positron emission tomography.

The prognosis of patients in our nonresectable group also differed significantly according to the presence of CTCs. Some authors have reported that response to chemotherapy can be evaluated in several cancers with distant metastasis. Monitoring the number of CTCs may be more useful for evaluating chemotherapy.[22,23] It is an advantage that the measurement of CTCs using the CellSearch system is available at any time and is easily and noninvasively performed. An increase in the number of CTCs should lead to a change in chemotherapy regimen.

The CellSearch system is based on the enumeration of epithelial cells, which are separated from the blood by EpCAM antibody-coated magnetic beads and identified with the use of fluorescently labeled antibodies against cytokeratin and with a fluorescent nuclear stain. In the detection of CTCs by molecular techniques there is always the question of whether the result could be a false-positive. Although Sensitivity of RT-PCR is very high for CTCs identification, it is impossible to visually confirm cancer cells. Conversely, with the Cell Search system (Janssen Diagnostics, LLC, Raritan, NJ), the false-positive rate is extremely low, because it is possible to morphologically confirm the presence of cells. Conversely, some cases might be missed (false-negative) because some of the CTCs may not express these epithelial markers and may be undetectable by the CellSearch system.[24]

Most reports concerning the prognosis for patients with breast cancer and prostate cancer have used a cutoff of $\geq$5 CTCs to determine a positive test.[12,13] Conversely, some reports of other cancers use different cutoff values.[25] The question remains regarding the significance of the presence of a single CTC. For patients with gastric cancer who have undergone curative resection, this single cell may be consequential. Our criteria defined $\geq$1 CTC as a positive test. It is important to note that CTCs were not detected in healthy volunteers in our series. In fact, several patients in our cohort who had only 1 CTC relapsed, and the presence of any CTCs in peripheral blood was considered an independent prognostic factor for determining the overall survival of patients who underwent gastrectomy. It may become possible to more accurately estimate the prognosis for these patients if the presence of CTCs is added to the staging factors. In this study, many patients who were positive for CTCs had a recurrence, and several patients who did not have a recurrence had received chemotherapy because of up-regulated serum tumor marker levels during follow-up. The detection of CTCs is useful for predicting recurrence and prognosis. We conclude that the evaluation of CTCs in peripheral blood may be a useful tool for predicting tumor progression, prognosis, and the effect of chemotherapy in patients with gastric cancer.

FUNDING SUPPORT

This work was supported in part by a grant-in-aid (no. 22501032) for scientific research from the Ministry of Education, Science, Sports, and Culture of Japan.

CONFLICT OF INTEREST DISCLOSURES

The authors made no disclosures.

REFERENCES

1. Yeh KH, Chen YC, Yeh SH, Chen CP, Lin JT, Cheng AL. Detection of circulating cancer cells by nested reverse transcription-polymerase chain reaction of cytokeratin-19 (K19)—possible clinical significance in advanced gastric cancer. *Anticancer Res.* 1998;18:1283-1286.
2. Noh YH, Kim JA, Lim GR, et al. Detection of circulating tumor cells in patients with gastrointestinal tract cancer using RT-PCR and its clinical implications. *Exp Mol Med.* 2001;33:8-14.
3. Vogel I, Kalthoff H. Disseminated tumour cells. Their detection and significance for prognosis of gastrointestinal and pancreatic carcinomas. *Virchows Arch.* 2001;439:109-117.
4. Ghossein RA, Bhattacharya S, Rosai J. Molecular detection of micrometastases and circulating tumor cells in solid tumors. *Clin Cancer Res.* 1999;5:1950-1960.
5. Nakashima S, Natsugoe S, Matsumoto M, et al. Clinical significance of circulating tumor cells in blood by molecular detection and tumor markers in esophageal cancer. *Surgery.* 2003;133:162-169.
6. Mimori K, Fukagawa T, Kosaka Y, et al. A large-scale study of MT1-MMP as a marker for isolated tumor cells in peripheral blood and bone marrow in gastric cancer cases. *Ann Surg Oncol.* 2008;15:2934-2942.
7. Bertazza L, Mocellin S, Marchet A, et al. Survivin gene levels in the peripheral blood of patients with gastric cancer independently predict survival [serial online]. *J Transl Med.* 2009;7:111.
8. Wu CH, Lin SR, Hsieh JS, et al. Molecular detection of disseminated tumor cells in the peripheral blood of patients with gastric cancer: evaluation of their prognostic significance. *Dis Markers.* 2006;22:103-109.
9. Mimori K, Fukagawa T, Kosaka Y, et al. Hematogenous metastasis in gastric cancer requires isolated tumor cells and expression of vascular endothelial growth factor receptor-1. *Clin Cancer Res.* 2008;14:2609-2616.
10. Koga T, Tokunaga E, Sumiyoshi Y, et al. Detection of circulating gastric cancer cells in peripheral blood using real time quantitative RT-PCR. *Hepatogastroenterology.* 2008;55:1131-1135.
11. Arigami T, Uenosono Y, Ishigami S, Hagihara T, Haraguchi N, Natsugoe S. Clinical significance of the B7-H4 coregulatory molecule as a novel prognostic marker in gastric cancer. *World J Surg.* 2011;35:2051-2057.
12. Cristofanilli M, Budd GT, Ellis MJ, et al. Circulating tumor cells, disease progression, and survival in metastatic breast cancer. *N Engl J Med.* 2004;351:781-791.
13. Leversha MA, Han J, Asgari Z, et al. Fluorescence in situ hybridization analysis of circulating tumor cells in metastatic prostate cancer. *Clin Cancer Res.* 2009;15:2091-2097.
14. Sobin LH, Gospodarowicz MK, Wittekind C, eds. TNM Classification of Malignant Tumours. 7th ed. Oxford, United Kingdom: Wiley-Blackwell; 2010.

15. Nishida S, Kitamura K, Ichikawa D, Koike H, Tani N, Yamagishi H. Molecular detection of disseminated cancer cells in the peripheral blood of patients with gastric cancer. *Anticancer Res.* 2000;20:2155-2159.
16. Ikeguchi M, Ohro S, Maeda Y, et al. Detection of cancer cells in the peripheral blood of gastric cancer patients. *Int J Mol Med.* 2003; 11:217-221.
17. Miyazono F, Natsugoe S, Takao S, et al. Surgical maneuvers enhance molecular detection of circulating tumor cells during gastric cancer surgery. *Ann Surg.* 2001;233:189-194.
18. Arigami T, Uenosono Y, Hirata M, Yanagita S, Ishigami S, Natsugoe S. B7-H3 expression in gastric cancer: a novel molecular blood marker for detecting circulating tumor cells. *Cancer Sci.* 2011; 102:1019-1024.
19. Saad AA, Awed NM, Abd Elkerim NN, et al. Prognostic significance of E-cadherin expression and peripheral blood micrometastasis in gastric carcinoma patients. *Ann Surg. Oncol.* 2010;17:3059-3067.
20. Sakuramoto S, Sasako M, Yamaguchi T, et al. Adjuvant chemotherapy for gastric cancer with S-1, an oral fluoropyrimidine. *N Engl J Med.* 2007;357:1810-1820.
21. Rahbari NN, Bork U, Kircher A, et al. Compartmental differences of circulating tumor cells in colorectal cancer. *Ann Surg Oncol.* 2012;19:2195-2202.
22. Budd GT, Cristofanilli M, Ellis MJ, et al. Circulating tumor cells versus imaging—predicting overall survival in metastatic breast cancer. *Clin Cancer Res.* 2006;12:6403-6409.
23. Nakamura S, Yagata H, Ohno S, et al. Multi-center study evaluating circulating tumor cells as a surrogate for response to treatment and overall survival in metastatic breast cancer. *Breast Cancer.* 2010;17:199-204.
24. Sakakura C, Hagiwara A, Nakanishi M, et al. Differential gene expression profiles of gastric cancer cells established from primary tumour and malignant ascites. *Br J Cancer.* 2002;87:1153-1161.
25. Hiraiwa K, Takeuchi H, Hasegawa H, et al. Clinical significance of circulating tumor cells in blood from patients with gastrointestinal cancers. *Ann Surg. Oncol.* 2008;15:3092-3100.

Bioconjugate Chemistry

Article

pubs.acs.org/bc

Cadmium-Free Sugar-Chain-Immobilized Fluorescent Nanoparticles Containing Low-Toxicity ZnS-$AgInS_2$ Cores for Probing Lectin and Cells

Hiroyuki Shinchi,[†] Masahiro Wakao,*[,†] Nonoka Nagata,[†] Masaya Sakamoto,[†] Eiko Mochizuki,[‡] Taro Uematsu,[‡] Susumu Kuwabata,[‡] and Yasuo Suda*[,†,§]

[†]Department of Chemistry, Biotechnology and Chemical Engineering, Graduate School of Science and Engineering, Kagoshima University, 1-21-40 Kohrimoto, Kagoshima 890-0065, Japan

[‡]Department of Applied Chemistry, Graduate School of Engineering, Osaka University, Suita, Osaka 565-0871, Japan

[§]SUDx-Biotec Corporation, 1-42-1 Shiroyama, Kagoshima 890-0013, Japan

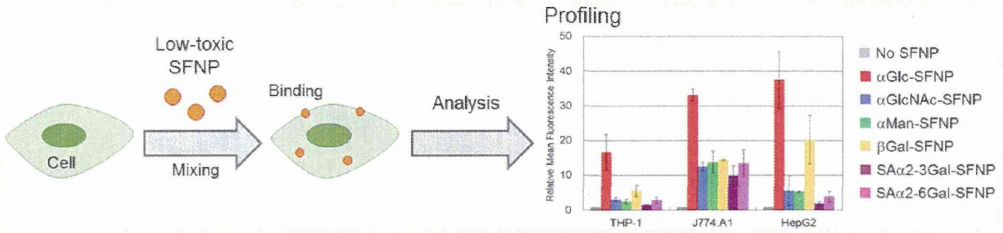

ABSTRACT: Sugar chains play a significant role in various biological processes through sugar chain−protein and sugar chain−sugar chain interactions. To date, various tools for analyzing sugar chains biofunctions have been developed. Fluorescent nanoparticles (FNPs) functionalized with carbohydrate, such as quantum dots (QDs), are an attractive imaging tool for analyzing carbohydrate biofunctions in vitro and in vivo. Most FNPs, however, consist of highly toxic elements such as cadmium, tellurium, selenium, and so on, causing problems in long-term bioimaging because of their cytotoxicity. In this study, we developed cadmium-free sugar-chain-immobilized fluorescent nanoparticles (SFNPs) using ZnS-$AgInS_2$ (ZAIS) solid solution nanoparticles (NPs) of low or negligible toxicity as core components, and investigated their bioavailability and cytotoxicity. SFNPs were prepared by mixing our originally developed sugar-chain-ligand conjugates with ZAIS/ZnS core/shell NPs. In binding experiments with lectin, the obtained ZAIS/ZnS SFNPs interacted with an appropriate lectin to give specific aggregates, and their binding interaction was visually and/or spectroscopically detected. In addition, these SFNPs were successfully utilized for cytometry analysis and cellular imaging in which the cell was found to possess different sugar-binding properties. The results of the cytotoxicity assay indicated that SFNPs containing ZAIS/ZnS have much lower toxicity than those containing cadmium. These data strongly suggest that our designed SFNPs can be widely utilized in various biosensing applications involved in carbohydrates.

INTRODUCTION

Cell-surface sugar chains play a significant role in a variety of biological events, such as cell−cell recognition, proliferation, differentiation, immune response, signal transduction, and infection.[1,2] The specific binding interaction between sugar chains and proteins, and sometimes between sugar chains and sugar chains, is the initiating point of these events. Analysis of the binding interaction at the molecular level therefore leads us not only toward a better understanding of these biofunctions, but also toward new biological insights involving sugar chains. Numerous efforts have been devoted to sugar-chain structure−function analysis, and many techniques like sugar chain array, chips, fluorescent probes, and nanoparticles have been developed.[3−22]

Nowadays, sugar chains are considered new biomarkers for determining cell type,[1,2,23−25] similar to nucleic acids and proteins,[26−28] since the glycosylation pattern on the cell surface varies depending on the tissue and cell type. Glycomic analysis of the cell is therefore a valuable approach for knowing cell status. Lectin-based profiling is a useful method for determining cell status and has been investigated in various cells like embryonic stem (ES) cells, induced pluripotent stem (iPS) cells, tumor cells, and other cultivated cell lines.[29−32] Sugar-chain-based profiling is a promising approach because the recognition ability of cells for sugar-chain changes depending on the cell conditions and provides information regarding the cell status, and is applicable to the evaluation of the metastatic property of tumor cells and quality control of cultivated cells.

Sugar-chain-immobilized fluorescent nanoparticles (SFNPs) are an attractive biosensing tool for the analysis of sugar chain

Received: September 17, 2013
Revised: January 14, 2014
Published: January 19, 2014

biofunctions.[16−22] Quantum dots (QDs) are often utilized as core components and have been extensively investigated as a fluorescent probe for biomedical imaging and diagnosis.[33−37] Therefore, various SFNPs containing QDs have been synthesized and their biological applications explored. Most QDs contains cadmium ions, which is often problematic in in vivo and/or in vitro bioassays because of their cytotoxic activity.[38−42] In order to suppress the cytotoxicity of cadmium ions, coating with a low-toxicity ZnS shell or various polymers has been utilized. However, it is difficult to completely abrogate the cytotoxicity of cadmium ions because these ions are released from nanoparticles by lysosomal degradation processes, photolysis, and oxidation.[39,43−46]

In this paper, we report the synthesis of cadmium-free SFNP using low-toxicity ZnS-$AgInS_2$ (ZAIS)/ZnS NPs. Immobilization of the sugar chain moiety was accomplished by a simple ligand exchange reaction using our ligand conjugates, in which various sugar-chain structures were conjugated with a thioctic acid moiety via a linker molecule. Carbohydrate−lectin interaction using our SFNPs was detected spectroscopically or visually. Flow cytometry analysis and fluorescent imaging of cells was also performed, and the results clarified that the binding property of cell for a sugar chain is different depending on the cell type. Furthermore, in the cytotoxicity assay, SFNPs containing ZAIS/ZnS NPs were found to be much less toxic than those containing CdTe/CdS QDs.

EXPERIMENTAL PROCEDURES

Materials. All chemical reagents were commercial grade except as noted. Thioglycolic acid (TGA, purity: 90%), 3-mercaptopropionic acid (3-MPA, purity: 98%), $NaBH_4$ (purity: >95.0%), KOH (purity: >85%), 3-(4,5-dimethylthiazol-2-yl)-2,5-diphenyltetrazolium bromide (MTT), and trypan blue solution (0.5%) were purchased from Nacalai Tesque (Kyoto, Japan). Thioacetamide (purity: >99.0%), zinc acetate anhydrate (purity: 99.99%), RPMI1640 medium, and Dulbecco's modified Eagle's medium (DMEM) were purchased from Sigma Aldrich (St. Louis, MO, USA). Indium(III) nitrate trihydrate (purity: >98.0%), silver nitrate (purity: 99.9%), sodium *N,N*-diethyldithiocarbamate trihydrate (purity: >90%), and zinc nitrate hexahydrate (99.9%) were purchased from Wako (Osaka, Japan). Oleylamine (purity: >40%) was purchased from TCI (Tokyo, Japan). Concanavalin A (Con A), *Ricin communis* agglutinin I (RCA120), and bovine serum albumin (BSA) were purchased from Seikagaku Corporation (Tokyo, Japan), Vector Laboratories (Burlingame, CA, USA), and Nacalai Tesque, respectively. Fetal bovine serum (FBS) was purchased from Nichirei (Tokyo, Japan). Penicillin streptomycin (PS) was purchased from GIBCO (Carlsbad, CA, USA). Milli-Q water (18.2 MΩ cm^{-1}) was used in all experiments unless otherwise noted. Sugar chain−ligand conjugates[47,48] and SFNPs containing CdTe/CdS[49] were prepared using previously reported methods.

Measurements. UV/vis spectra and fluorescence spectra were measured using a V-650 spectrometer and an FP-6310 fluorescence spectrometer (JASCO, Tokyo, Japan), respectively. Mass spectra were measured using the Voyager-DE-PRO (Applied Biosystems, Foster City, CA, USA) or micrOTOF II (Bruker Daltonics, Billerica, MA, USA). Flow cytometry analyses were performed using the Cytomics FC 500 Cytometer (Beckman Coulter, Brea, CA, USA). Fluorescence imaging data were obtained using a Nikon A1si-90i (Nikon, Tokyo, Japan). Colorimetric MTT assay was performed using an Immuno Mini NJ-2300 (MICROTEC, Chiba, Japan). Stained cells were observed using an inverted microscope CKX-31 (Olympus, Tokyo, Japan).

Preparation of Sugar-Chain−Ligand Conjugates. Sugar-chain−ligand conjugates were prepared by the method reported previously.[47,48] Oligosaccharides used were commercially available or from a synthetic source. Briefly, a mixture of oligosaccharide and linker moiety in DMAc/H_2O/AcOH (10:10:1) was left at 40 °C. After 5 h, $NaBH_3CN$ was added to the mixture and the reaction mixture was left at 40 °C again. After 3 days, the reaction mixture was lyophilized. The residue was then purified by reversed-phase silica gel column chromatography (eluent: H_2O/MeOH gradient system) to yield the sugar-chain−ligand conjugate.

***N*-[3-[(2-Deoxy-2-acetamido-α-D-glucopyranosyl)-(1−4)-(1-deoxy-D-glucitol-1-yl)amino]phenyl]-DL-α-lipoamide (GlcNAcα1−6Glc-mono, 3).** ^{1}H NMR (600 MHz, D_2O) δ 7.019 (1H, t, *J* = 8.2 Hz, aromatic), 6.78 (1H, s, aromatic), 6.65 (1H, d, *J* = 8.2 Hz, aromatic), 6.38 (1H, d, *J* = 8.2 Hz, aromatic), 4.61 (1H, d, $J_{1',2'}$ = 3.4 Hz, H-1′), 3.76 (1H, ddd, $J_{2,3}$ = 6.8 Hz, $J_{2,1a}$ = 5.4 Hz, $J_{2,1b}$ = 4.8 Hz, H-2), 3.73−3.60 (5H, m, H-3, H-5, H-6a, H-2′, H-6a′), 3.55−3.49 (5H, m, H-4, H-3′, H-5′, H-6b′, -SSCH$_2$CH$_2$C$\underline{H}$=), 3.39 (1H, d, $J_{6a,6b}$ = 8.2 Hz, H-6b), 3.23 (1H, dd, $J_{4',3'}$ = 8.8 Hz, $J_{4',5'}$ = 9.5 Hz, H-4′), 3.17 (1H, dd, $J_{1a,2}$ = 4.8 Hz, $J_{1a,1b}$ = 8.8 Hz, H-1a), 3.07 (1H, ddd, *J* = 10.7 Hz, 6.1 Hz, 6.1 Hz, -SSC$\underline{H}_2$CH$_2$CH=), 3.01 (1H, ddd, *J* = 11.3 Hz, 6.8 Hz, 6.1 Hz, -SSC$\underline{H}_2$CH$_2$CH=), 2.94 (1H, dd, $J_{1b,2}$ = 5.4 Hz, $J_{1b,1a}$ = 8.2 Hz, H-1b), 2.32 (1H, dddd, *J* = 12.7 Hz, 6.1 Hz, 6.1 Hz, 6.1 Hz, -SSCH$_2$C$\underline{H}_2$CH=), 2.22 (2H, t, *J* = 7.48 Hz, -NHCOC$\underline{H}_2$-), 1.83 (3H, s, −COC$\underline{H}_3$), 1.82−1.78 (1H, m, -SSCH$_2$C$\underline{H}_2$CH=), 1.64−1.59 (1H, m, -NHCOCH$_2$C$\underline{H}_2$-), 1.55−1.44 (3H, m, -NHCOCH$_2$C$\underline{H}_2$-, -NHCOCH$_2$CH$_2$CH$_2$C$\underline{H}_2$-), 1.34−1.27 (2H, m, -NHCOCH$_2$CH$_2$C$\underline{H}_2$-); HRMS (positive mode); Found: *m*/*z* 686.2391 [(M+Na)$^+$], Calcd. for $C_{26}H_{42}N_2O_{11}S_2Na$: 686.2388.

***N*-[3-[(α-D-Mannopyranosyl)-(1−4)-(1-deoxy-D-glucitol-1-yl)amino]phenyl]-DL-α-lipoamide (Manα1−6Glc-mono, 4).** ^{1}H NMR (600 MHz, D_2O) δ 7.20 (1H, t, *J* = 8.2 Hz, aromatic), 6.95 (1H, s, aromatic), 6.85 (1H, *J* = 7.5 Hz, d, aromatic), 6.58 (1H, d, *J* = 7.5 Hz, aromatic), 4.82 (1H, s, H-1′), 3.97−3.92 (1H, ddd, $J_{2,3}$ = 7.7 Hz, $J_{2,1a}$ = 4.1 Hz, $J_{2,1b}$ = 4.1 Hz, H-2), 3.92−3.88 (1H, m, H-2′), 3.88−3.80 (4H, m, H-3, H-6a, H-6a′, H-6b′), 3.80−3.76 (1H, dd, $J_{3',4'}$ = 6.1 Hz, $J_{3',2'}$ = 3.4 Hz, H-3′), 3.73−3.59 (6H, m, H-4, H-5, H-6b, H-4′, H-5′, -SSCH$_2$CH$_2$C$\underline{H}$=), 3.35 (1H, dd, $J_{1a,2}$ = 4.1 Hz, $J_{1a,1b}$ = 9.5, H-1a), 3.25 (1H, ddd, *J* = 10.1 Hz, 6.8 Hz, 6.8 Hz, -SSC$\underline{H}_2$CH$_2$CH=), 3.19 (1H, ddd, *J* = 10.1 Hz, 6.8 Hz, 6.8 Hz, -SSC$\underline{H}_2$CH$_2$CH=), 3.16−3.11 (1H, dd, $J_{1b,1a}$ = 8.2 Hz, $J_{1b,2}$ = 5.4 Hz, H-1b), 2.50 (1H, dddd, *J* = 12.3 Hz, 6.1 Hz, 6.1 Hz, 6.1 Hz, -SSCH$_2$C$\underline{H}_2$CH=), 2.40 (2H, t, *J* = 6.8 Hz, -NHCOC$\underline{H}_2$-), 2.00 (1H, dddd, J = 12.3 Hz, 6.1 Hz, 6.1 Hz, 6.1 Hz, -SSCH$_2$C$\underline{H}_2$CH=), 1.82−1.76 (1H, m, -NHCOCH$_2$C$\underline{H}_2$-), 1.76−1.64 (3H, m, -NHCOCH$_2$C$\underline{H}_2$-, -NHCOCH$_2$CH$_2$CH$_2$C$\underline{H}_2$-), 1.53−1.47 (2H, m, -NHCOCH$_2$CH$_2$C$\underline{H}_2$-); HRMS (positive mode); Found: *m*/*z* 645.2126 [(M+Na)$^+$], Calcd. for $C_{26}H_{42}N_2O_{11}S_2Na$: 645.2122.

***N*-[3-[(5-Acetamido-3,5-dideoxy-D-*glycero*-α-D-galacto-2-nonulopyranosidonic acid)-(2−3)-(α-D-galactopyranosyl)-(1−4)-(1-deoxy-D-glucitol-1-yl)amino]phenyl]-DL-α-lipoamide (SAα2−3Galβ1−4Glc-mono, 5).** ^{1}H NMR (600 MHz, D_2O) δ 7.40 (1H, t, *J* = 8.2 Hz, aromatic), 7.34

dx.doi.org/10.1021/bc400425w | *Bioconjugate Chem.* 2014, 25, 286−295

(1H, s, aromatic), 7.21 (1H, d, J = 8.2 Hz, aromatic), 6.90 (1H, d, J = 8.2 Hz), 7.41−6.90 (4H, m, aromatic), 4.58 (1H, dd, $J_{1',2'}$ = 7.5 Hz, H-1′), 4.09−4.08 (2H, m, H-2, H-3′), 3.96−3.58 (18H, m, H-3, H-4, H-5, H-6a, H-6b, H-2′, H-4′, H-5′, H-6a′, H-6b′, H-4″, H-5″, H-6″, H-7″, H-8″, H-9a″, H-9b″, -SSCH$_2$CH$_2$CH=), 3.52−3.49 (1H, m, H-1a), 3.37−3.26 (2H, m, H-1b, -SSCH$_2$CH$_2$CH=), 3.23 (1H, ddd, J = 11.3 Hz, 6.8 Hz, 6.8 Hz, -SSCH$_2$CH$_2$CH=), 2.78−2.76 (1H, m, H-3a″), 2.59−2.52 (1H, m, -NHCOCH$_2$CH$_2$-), 2.47 (2H, t, J = 6.8 Hz, NHCOCH$_2$CH$_2$), 2.06 (3H, s, −COCH$_3$), 2.05−2.01 (1H, m, -SSCH$_2$CH$_2$CH=), 1.83−1.71 (5H, m, H-3b″, -NHCOCH$_2$CH$_2$-, -NHCOCH$_2$CH$_2$CH$_2$CH$_2$-), 1.55−1.53 (2H, m, -NHCOCH$_2$CH$_2$CH$_2$-); ESI-MS (positive mode); Found: m/z 958.2894 [(M+2Na)$^+$], Calcd. for $C_{37}H_{58}N_3O_{19}S_2Na_2$: 958.2896.

***N*-[3-[(5-Acetamido-3,5-dideoxy-D-*glycero*-α-D-galacto-2-nonulopyranosidonic acid)-(2−6)-(α-D-galactopyranosyl)-(1−4)-(1-deoxy-D-glucitol-1-yl)amino]phenyl]-DL-α-lipoamide (SAα2−6Galβ1−4Glc-mono, 6).** ^{1}H NMR (600 MHz, D$_2$O) δ 7.28 (1H, t, J = 7.5 Hz, aromatic), 7.25−7.23 (2H, m, aromatic), 6.71 (1H, d, J = 6.8 Hz, aromatic), 4.47 (1H, d, $J_{1',2'}$ = 8.2 Hz, H-1′), 4.04 (1H, m, H-2), 3.93−3.52 (19H, m, H-3, H-4, H-5, H-6a, H-6b, H-2′, H-3′, H-4′, H-5′, H-6a′, H-6b′, H-4″, H-5″, H-6″, H-7″, H-8″, H-9a″, H-9b″ -SSCH$_2$CH$_2$CH=), 3.43 (1H, dd, $J_{1a,1b}$ = 8.8 Hz, $J_{1a,2}$ = 4.1 Hz, H-1a), 3.31−3.29 (2H, m, H-1b, -SSCH$_2$CH$_2$CH=), 3.24 (1H, ddd, J = 10.7 Hz, 6.8 Hz, 6.1 Hz, -SSCH$_2$CH$_2$CH=), 2.75−2.72 (1H, m, H-3a″), 2.55 (1H, dddd, J = 12.3 Hz, 6.1 Hz, 6.1 Hz, 6.1 Hz, -SSCH$_2$CH$_2$CH=), 2.45 (2H, t, J = 6.8 Hz, -NHCOCH$_2$-), 2.06 (3H, s, −COCH$_3$), 2.04−2.02 (1H, m, -NHCOCH$_2$CH$_2$-), 1.82−1.76 (1H, m, -NHCOCH$_2$CH$_2$-), 1.86−1.69 (4H, m, H-3b″, -NHCOCH$_2$CH$_2$-, -NHCOCH$_2$CH$_2$CH$_2$-), 1.55−1.53 (2H, m, -NHCOCH$_2$CH$_2$CH$_2$-); HRMS (positive mode); Found: m/z 958.2892 [(M+2Na)$^+$], Calcd. for $C_{37}H_{58}N_3O_{19}S_2Na_2$: 958.2896.

Preparation of ZAIS/ZnS NPs. Hydrophobic ZAIS/ZnS core/shell NPs were prepared according to the method reported by Torimoto et al.[50,51] The ZAIS core were prepared by thermal decomposition of a metal ion-diethyldithiocarbamate complex of $(AgIn)_xZn_{2(1-x)}(S_2CN(C_2H_5)_2)_4$. Briefly, the complex powder was prepared by mixing 50 mL of a sodium diethyldithiocarbamate aqueous solution (50 mM) with 50 mL of an aqueous solution containing silver nitrate, indium nitrate, and zinc nitrate at a molar ratio of x:x:2(1 − x) (total concentration of metal ions: 25 mM) followed by washing with methanol several times and drying under vacuum. The complex powder (50.0 mg) was placed in a two-necked flask and heat-treated at 180 °C for 30 min in Ar atmosphere. Then, oleylamine (3 mL) was added to the obtained brown powder, followed by further heat treatment under vigorous stirring at 180 °C for 5 min in Ar atmosphere. The resulting suspension was subjected to centrifugation (4000 × g, 5 min) to remove large particles. ZAIS NPs were precipitated by the addition of methanol. Oleylamine (2 mL) was then added to the obtained precipitates. After the appropriate amounts of zinc acetate and thioacetamide at a molar ratio of 1:1 (x = 0.9: 56.3 μmol; x = 0.6: 46.1 μmol; x = 0.4: 34.8 μmol) were added, the mixture was heated at 180 °C for 30 min in Ar atmosphere to cover with the ZnS shell. The ZAIS/ZnS core/shell NPs were precipitated by the addition of methanol. The wet precipitates were dissolved in chloroform (12 mL) to give a solution of hydrophobic ZAIS/ZnS NPs.

Next, hydrophobic NPs were converted to hydrophilic NPs. To a mixture of 3-MPA solution in ethanol (200 mM, 1 mL) and KOH solution in ethanol (300 mM, 1 mL) the NPs chloroform solution (2 mL) was added at 0 °C. The mixture was then stirred at the same temperature for 3 h in the dark. The resulting precipitates were collected by centrifugal separation (4000 × g, 5 min). The precipitates were dissolved in water (2.0 mg/mL). The concentration of NPs was estimated from the absorbance at 360 nm. The obtained hydrophilic 3-MPA-capped ZAIS/ZnS NPs were treated with a solution of zinc acetate, thioacetamide, and TGA, sequentially. Zinc acetate, thioacetamide, and TGA were dissolved in water (2 mL) at a molar ratio of 1:1:1 (x = 0.9: 56.3 μmol; x = 0.6: 46.1 μmol; x = 0.4: 34.8 μmol). The pH of the mixture was adjusted to 9 with NaOH (1.0 M). The hydrophilic ZAIS/ZnS NPs solution (2 mL) was added to the mixture. The reaction mixture was stirred and heated at 80 °C for 5 h under open-air conditions. After cooling, the resulting solution was diluted with water and its concentration adjusted to 0.5 mg/mL.

Immobilization of Sugar Chain onto ZAIS/ZnS NPs. The solution of ZAIS/ZnS NPs (0.5 mg/mL, 200 μL) was concentrated by centrifugal filtration (12 000 × g, 5 min) using an Amicon Ultra 10K (Millipore, Billerica, MA, USA). The NPs were washed with water (100 μL × 2) and resuspended in water (100 μL). In another microtube, sugar chain−ligand conjugates (50 mM, 50 μL) and NaBH$_4$ aq. solution (500 mM, 50 μL,) were mixed at room temperature and the mixture was left for 10 min. The obtained solutions (each 100 μL) were then mixed and heated for 2 h in the dark at 50 °C. Excess unreacted ligand conjugates were removed by centrifugal filtration (14 000 × g, 5 min) using an Amicon Ultra 10K, and the residue was washed with water 3 times; then, PBS was added to prepare the SFNP solution.

Analysis of the Interaction between Proteins and Sugar Chains on SFNPs. The proteins, Con A, RCA120, or BSA, dissolved in PBS, were diluted sequentially. Fifty microliters of the resulting protein solution (20 μM) was placed in each well of a 96-well plate. Fifty microliters of the colloidal solution (0.5 mg/mL) was then added to the wells containing the 20 μM protein solution. After gentle agitation for 1 h, the fluorescent spectrum of the supernatant from each well was measured.

Uptake of SFNPs into Cells. THP-1 cells were placed in a cell culture flask (BD Falcon, Franklin Lakes, NJ, USA) and cultivated at 37 °C under 5% CO_2 in RPMI1640 medium containing 10% FBS and 1% PS. J774.A1 cells and HepG2 cells were placed in a cell culture flask and cultivated at 37 °C under 5% CO_2 in DMEM containing 10% FBS and 1% PS, respectively. HepG2 cells were subcultured when monolayers were 70% confluent by treatment with 0.05% trypsin containing 2 mM EDTA and then collected. For flow cytometry analysis using THP-1 and J774.A1, 5 × 10^5 cells (1 mL) were placed in microtubes and incubated in 150 μL of fresh medium (FBS- and PS-free) containing SFNPs (concentration: 100 μg/mL). After 3 h incubation at 37 or 4 °C, the medium was removed. The cells were washed with PBS (1 mL) 3 times and subjected to flow cytometry analysis. In the case of HepG2, 5 × 10^5 cells were placed in 12-well plate and incubated at 37 °C. After 48 h incubation, the medium was removed and 350 μL of fresh medium (FBS- and PS-free) containing SFNPs (concentration: 100 μg/mL) were added. After incubation for an additional 3 h at 37 or 4 °C, the medium was removed. The cells were washed with PBS (1 mL) 3 times, collected by a cell scraper (Iwaki,

Tokyo, Japan), and subjected to flow cytometry analysis. Data were accumulated using a FACS cytometer (Cytomics FC500 Cytometer). The excitation wavelength was 488 nm. Cells were gated for living cells. Fluorescence channel FL-4 was used to detect SFNP uptake by the cells. For microscopic imaging, 5×10^4 HepG2 cells were seeded in 8-well glass chamber slides. After 48 h incubation at 37 °C, the medium was removed and 100 μL of fresh medium (FBS- and PS-free) containing SFNPs (100 μg/mL) was added. After 3 h incubation at 37 °C, the cells were washed with PBS 3 times and a coverslip was placed on top of the cells. The slides were immediately observed using confocal laser scanning microscopy.

Cytotoxicity Assay of SFNPs. The cytotoxicity of SFNPs was evaluated by the MTT assay[52] and trypan blue assay with ZAIS/ZnS SFNPs and CdTe/CdS SFNPs. For the MTT assay, 1×10^5 HepG2 cells (1 mL) were placed in a 24-well plate and cultivated at 37 °C under 5% CO_2 for 24 h. The cells were then placed in fresh medium (200 μL) containing various concentrations of SFNPs (5, 25, 50, 100 μg/mL). After 24 h incubation, the cells were washed with PBS (200 μL × 3). One hundred microliters of MTT solution (5 mg/mL) were added to each well and incubated for an additional 4 h at 37 °C. The medium was removed and 1 mL of DMSO was added to each well to dissolve the MTT formazan product. After agitating for 1 h, the supernatant was recovered and the amount of MTT formazan was determined by measuring the absorbance at 540 nm using Immuno Mini NJ-2300.

For the trypan blue assay, 1×10^6 J774.A1 cells were placed in a microtube and incubated in fresh medium (200 μL) containing various concentrations of SFNPs (5, 25, 50, 100, 250 μg/mL). After 24 h incubation, 10 μL of cell suspension were transferred to a 200 μL microtube and incubated for 3 min at room temperature with an equal volume of 0.5% (w/v) trypan blue staining solution. The percentage of cell viability was determined by microscopic observation using an Olympus CKX-31 microscope with a dual-chamber hemocytometer.

For the observation of cellular morphology, 1×10^5 HepG2 cells (200 μL) were placed in 8-well glass chamber slides and cultivated for 48 h at 37 °C. The cells were placed in fresh medium (200 μL) containing various concentrations of SFNPs (5, 50 μg/mL). After 24 h incubation at 37 °C, the cells were washed with PBS (200 μL × 3), treated with a 4% formaldehyde aqueous solution for 15 min at 4 °C, and washed with PBS (200 μL × 3) again. Microscopic images were obtained using Eclipse 90i.

■ RESULTS AND DISCUSSION

Preparation of SFNPs Containing ZAIS/ZnS. Several methods for the preparation of cadmium-free fluorescent nanoparticles, such as ZnS,[53] $CuInS_2$,[54−56] ZAIS,[50,51] and InP,[57,58] have been reported. In particular, ZAIS/ZnS core/shell NPs reported by Torimoto and co-workers showed attractive optical properties and high quantum yields (up to 80%). In addition, the emission color is tunable from green to red depending on their chemical composition, and no highly toxic element was contained in their components.

The chemical formula of ZAIS is $Zn_{2(1-x)}(AgIn)_xS_2$. The photoluminescence property of ZAIS is controllable by changing the x value. In this study, we prepared ZAIS NPs with $x = 0.9$, which gives an emission peak at around 650 nm (excitation wavelength: 360 nm). The synthesis of ZAIS/ZnS core−shell NPs was carried out according to the method reported by Torimoto and co-workers, in which oleylamine was temporally coated on the NP surface.[50,51] The hydrophobic oleylamine-coated ZAIS/ZnS NPs were then converted to hydrophilic NPs by treatment with 3-MPA in EtOH, followed by sequential treatment with zinc acetate, thioacetamide, and thioglutaric acid (TGA) in water at 80 °C, affording TGA-capped ZAIS/ZnS NPs. Immobilization of sugar chains onto TGA-capped ZAIS/ZnS NPs was performed by a simple ligand-exchange reaction using our original sugar chain−ligand conjugates under reductive conditions with $NaBH_4$ (Figure 1).[49] The optimum concentration of sugar chain−ligand

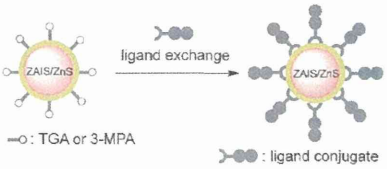

Figure 1. Preparation of SFNPs.

conjugate was examined with Glcα1−4Glc-mono ligand conjugates (**1**), which exhibited a plateau at 10−12.5 mM of the ligand conjugate (Figure 2A). The number of sugar-chain molecules per particle was estimated to be about 320 by analysis using the anthrone-sulfuric acid method,[59] which was higher than the theoretical value[60] (the number of thioctic acid as a bidentate ligand: 130 per particle; particle diameter: 4.0 nm). It is strongly suggested that most of the ligand conjugates monovalently bind to the NP surface by the treatment of excess amounts of ligand conjugates. Immobilization of the sugar moiety was qualitatively confirmed by matrix-assisted laser desorption ionization time-of-flight mass spectrometry (MALDI-TOF MS) analysis as shown in Figure 2B. A corresponding mass peak (m/z) of the used ligand conjugate was observed. The size of the obtained SFNPs was determined by transmission electron microscopy (TEM) and dynamic light scattering (DLS) analysis (Figure 2C and D). Other ligand conjugates (Galβ1−4Glc-mono [**2**], GlcNAcα1−6Glc-mono [**3**], Manα1−6Glc-mono [**4**], SAα2−3Galβ1−4Glc-mono [**5**], and SAα2−6Galβ1−4Glc-mono [**6**]) (Figure 3) were used for similarly immobilizing sugar chains onto ZAIS/ZnS NPs. All these SFNPs exhibited significant stability and high dispersibility in water or phosphate-buffered saline (PBS). Lyophilized SFNPs could be stored for at least several months in a cold chamber under dark conditions (data not shown).

Binding Experiments of SFNPs with Lectins. It is known that the interaction between sugar-chain immobilized nanoparticles and proteins possessing multiple sugar-binding sites yields aggregates and can be detected visually and spectroscopically.[19,49,61] The binding analysis of SFNPs containing ZAIS/ZnS NPs with proteins was shown in Figure 4. The proteins used were Con A (α-glucose- and α-mannose-specific), RCA120 (β-galactose-specific), and BSA (no specific binding to sugar chain). In the case of SFNPs immobilized with αGlc (αGlc-SFNP), aggregates were obtained only in the case of Con A, but not with RCA120 or BSA. When SFNPs immobilized with αGlcNAc (αGlcNAc-SFNP) were used, aggregates occurred similarly to the case of αGlc-SFNP. This result is reasonable in that the functional group at the 2-position on α-gluco- or α-mannopyranose ring does not affect the recognition of Con A. In the case of SFNPs immobilized with βGal (βGal-SFNP), aggregates were obtained in the case of RCA120, but not with Con A or BSA. On the other hand,

dx.doi.org/10.1021/bc400425w | Bioconjugate Chem. 2014, 25, 286−295

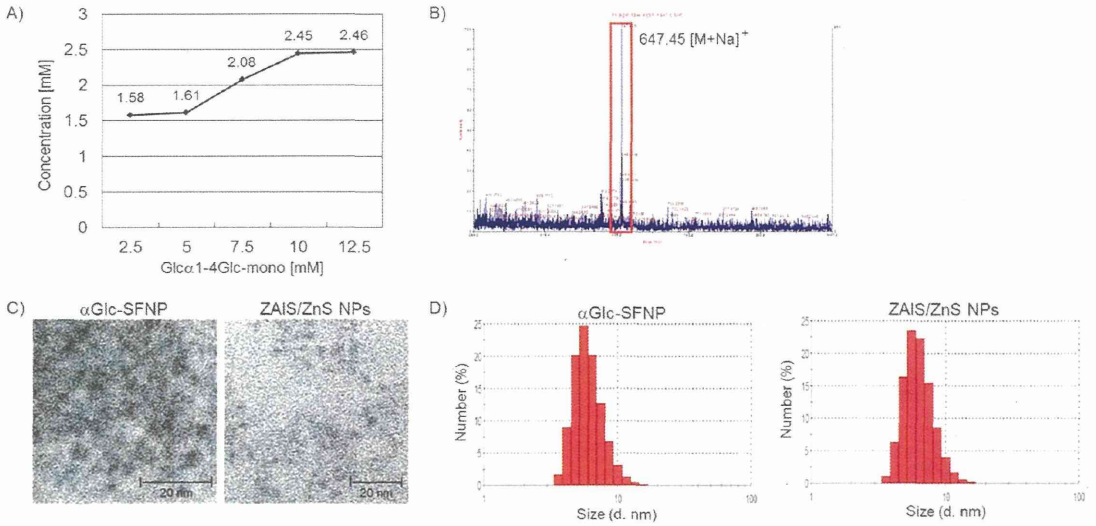

Figure 2. (A) Ligand exchange reaction under various concentrations of **1**. (B) MS analysis of SFNPs prepared with **1**. The detected peak was 647.45 $[M+Na]^+$. (C) TEM imaging of SFNPs ($x = 0.9$) prepared with **1** and ZAIS/ZnS ($x = 0.9$) NPs stabilized with TGA. The average diameter was about 4.0 nm. Scale bar: 20 nm. (D) Histogram of DLS data of SFNPs prepared using Glcα1−4Glc-mono and NPs stabilized with TGA. Average hydrodynamic diameter was about 6.2 nm.

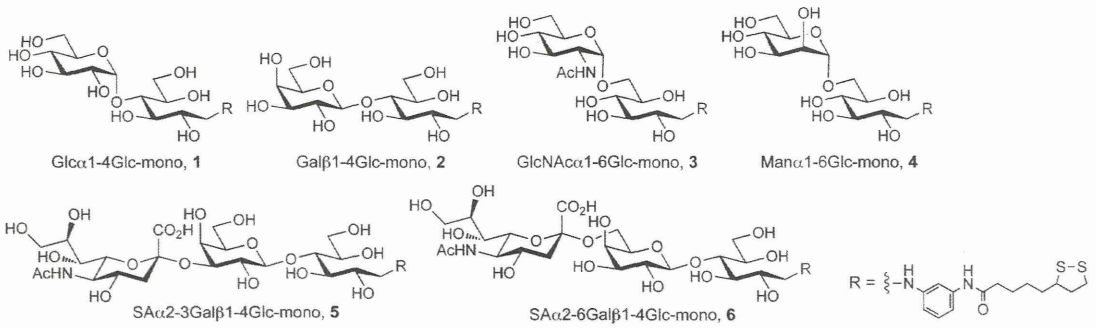

Figure 3. Sugar-chain−ligand conjugates used in this study.

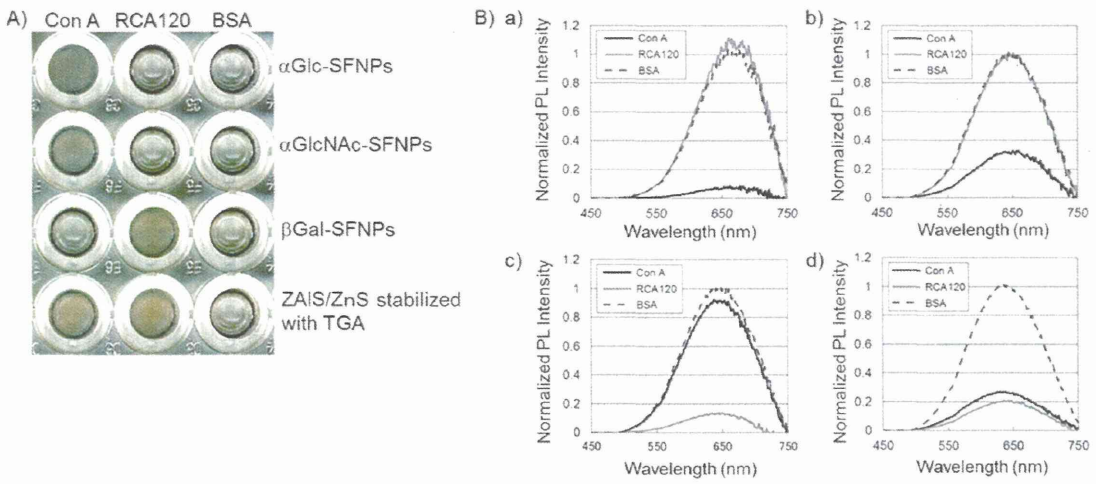

Figure 4. Interaction analysis between SFNPs and proteins. (A) Visual image. Each SFNPs was mixed with protein. (B) The fluorescent spectrum of supernatant monitored by excitation wavelength at 400 nm. (a) αGlc-SFNP, (b) αGlcNAc-SFNP, (c) βGal-SFNP, (d) ZAIS/ZnS stabilized with TGA.

dx.doi.org/10.1021/bc400425w | Bioconjugate Chem. 2014, 25, 286−295

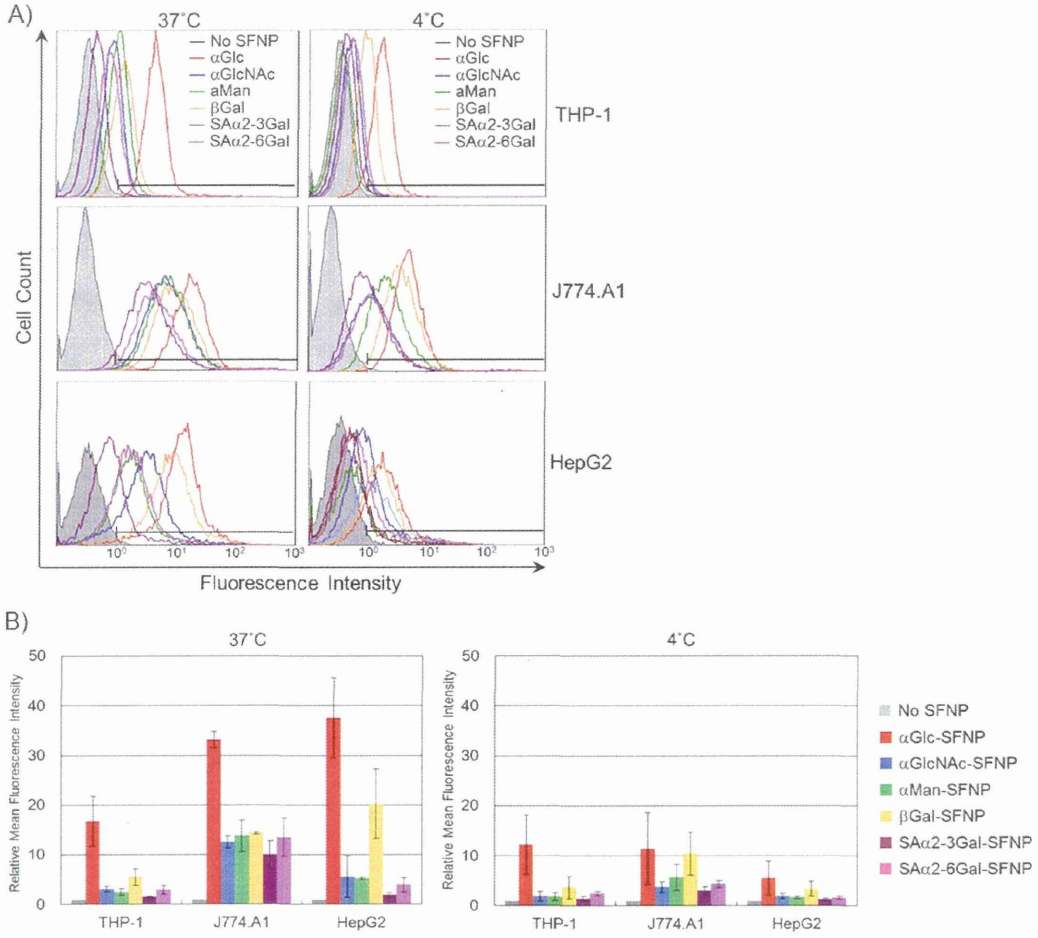

Figure 5. Flow cytometry analysis. The histogram of each cell incubated at 37 °C (left) or 4 °C (right) (A) and relative mean fluorescence intensity (MFI, B). The excitation wavelength in the FACS experiment was 488 nm. Cells were gated on living cells and FL-4 was used as a fluorescence channel to detect each cell labeled with SFNPs.

when TGA capped ZAIS/ZnS NPs were mixed with protein, aggregates were formed in both case of Con A and RCA120, indicating nonspecific binding. In fluorescent spectra, a decrease in the fluorescent intensity of the supernatant was observed (Figure 4B) due to the specific binding of protein to SGNPs. Thus, SFNPs containing ZAIS/ZnS NPs are applicable for both visual and fluorescent detection of sugar chain−protein interaction, the same as SFNPs containing CdTe/CdS.

Cellular Uptake of SFNPs. Following the successful binding experiments of SFNPs with proteins, the SFNPs were applied to cellular labeling and imaging. Various sugar chain-binding receptor proteins are expressed on the cell surface. The evaluation of the sugar chain-binding properties of the cell provides functional information on the cell and classifies the cell type. In the binding experiments, 3 kinds of cell lines, a human acute monocytic leukemia cell line (THP-1), a murine macrophage cell line (J774.A1), and a human hepatic carcinoma cell line (HepG2), and 6 kinds of SFNPs, αGlc-SFNP, βGal-SFNP, αGlcNAc-SFNP, αMan-FNP (FNPs with immobilized **4**), SAα2−3Gal-SFNP (FNPs with immobilized **5**), and SAα2−6Gal-SFNP (FNPs immobilizing **6**) were used. The results of flow cytometry analysis are shown in Figure 5. Mean fluorescence intensity (MFI) was calculated from fluorescence intensity per cell. The relative MFI value was calculated based on the value when cells were incubated without SFNPs. After 3 h of incubation, different cellular uptake of SFNPs was observed on the basis of the sugar-chain type. αGlc-SFNPs were found to bind to all 3 types of cell lines. This binding may occur by the interaction with the glucose transporter, since cells express the protein on the surface to take up glucose as an energy source.[62] In the binding analysis with THP-1 cells, the SFNPs, except those with αGlc, showed low affinity compared to that seen with other cells. THP-1 cells are known to be immature hematopoietic cells and may not express enough amounts of sugar-binding receptors. On the other hand, J774.A1 cells, mature macrophage cells, showed high binding affinities for all the SFNPs. Mature macrophage cells are known to express various sugar-chain binding receptors such as mannose-binding protein (MBP),[63] galectin (galactose-binding protein),[64,65] and sialoadhesin (sialic acid-binding protein).[66,67] The two former receptors are involved in the phagocytotic clearance of microorganisms. The latter is related to their migration and infiltration. In the case of HepG2 cells, βGal-SFNP predominantly bound to the cells. Hepatic cells normally express asialoglycoprotein receptor,[68−71] which recognizes the terminal galactose moiety to remove asialogly-

dx.doi.org/10.1021/bc400425w | Bioconjugate Chem. 2014, 25, 286−295

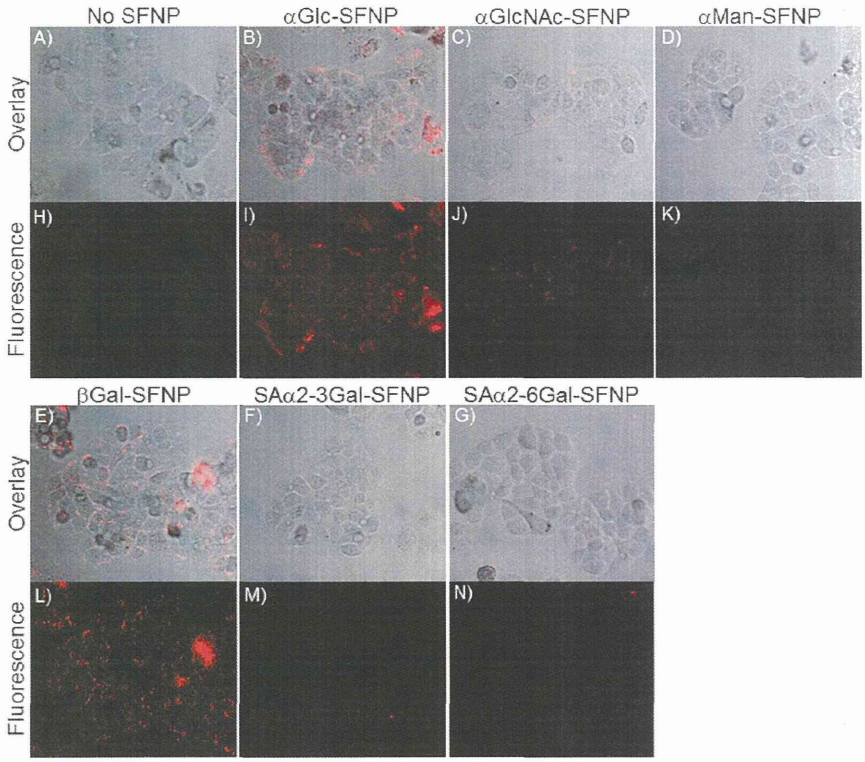

Figure 6. Confocal laser scanning microscopic imaging of HepG2 cells. Overlay images (top panel, A–G) and fluorescence images (lower panel H–N). HepG2 cells were incubated without SFNPs (A and H) and with αGlc-SFNPs (B and I), αGlcNAc-SFNPs (C and J), βGal-SFNPs (D and K), SAα2–3Gal-SFNPs (F and M), or SAα2–6Gal-SFNPs (G and N).

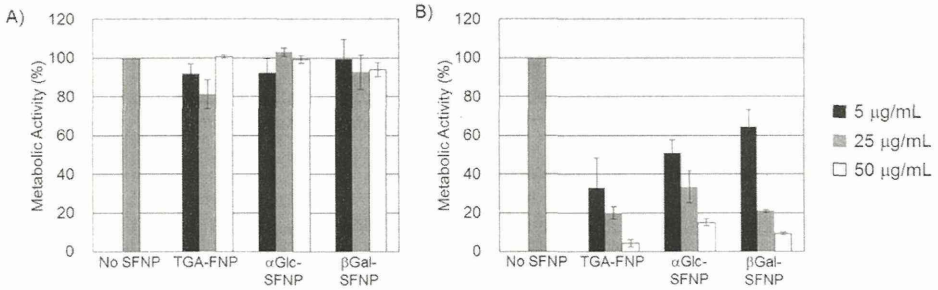

Figure 7. MTT assay for SFNPs. HepG2 cells were incubated with ZAIS/ZnS NPs (A) or CdTe/CdS QDs (B). The nanoparticle concentration was in the range of 5 μg/mL to 50 μg/mL (left to right).

coproteins. On the other hand, the binding intensity of the cells incubated at 4 °C was significantly decreased compared with cells incubated at 37 °C. These results indicate that SFNPs not only bound to the cell surface but were also internalized into the cells by endocytosis. Confocal laser scanning imaging for HepG2 cells yielded results similar to that of fluorescent-activated cell sorting (FACS) analysis, which showed that αGlc-SFNP and βGal-SFNP were predominantly taken up while αGlcNAc-SFNP, SAα2–3Gal-SFNP, and SAα2–6Gal-SFNP were only slightly taken up (Figure 6). Thus, our prepared SFNPs are useful for the analysis and imaging of cells on the basis of sugar chain–protein interactions, and can be applicable to cell profiling.

Cytotoxicity Assay of SFNPs. The cytotoxic activity of SFNPs was evaluated by the MTT assay and morphological analysis. In this assay, HepG2 cells were used. CdTe/CdS QDs were used for comparing cytotoxicity. In addition, to investigate the effect of capping agents, three kinds of capping agents, **1**, **2**, and TGA, were used. TGA-capped CdTe/CdS QDss and CdTe/CdS SFNPs were prepared according to our previous method.[49] The results of the MTT assay after 24 h incubation are shown in Figure 7. Interestingly, the metabolic activity of cells treated with ZAIS/ZnS NPs was similar to that of untreated cells (Figure 7A). The morphology of cells treated with ZAIS/ZnS SFNPs was also the same as that of untreated cells (Figure 8D and E). These data indicate that ZAIS/ZnS NPs were nontoxic in the concentration range of 5–50 μg/mL. On the other hand, treatment with CdTe/CdS SFNPs dramatically decreased metabolic activity (Figure 7B), although capping of the QDs with sugar-chain–ligand conjugates such as

dx.doi.org/10.1021/bc400425w | Bioconjugate Chem. 2014, 25, 286–295